PHYSICAL REVIEW B **85**, 201416(R) (2012)

Dynamic probe of atom exchange during monolayer growth

O. Moutanabbir,[1,2,3,*] F. Ratto,[4] S. Heun,[5] K. Scheerschmidt,[2] A. Locatelli,[6] and F. Rosei[7]

[1]*Département de Génie Physique, École Polytechnique de Montréal, Montréal, Case Postale 6079, Succursale Centre-Ville, Montréal, Québec, Canada H3C 3A7*

[2]*Max Planck Institute of Microstructure Physics, Weinberg 2, 06120 Halle (Saale), Germany*

[3]*School of Fundamental Science and Technology, Keio University, 3-14-1 Hiyoshi, Kohoku-ku, Yokohama 223-8522, Japan*

[4]*Istituto di Fisica Applicata, Consiglio Nazionale delle Ricerche (CNR-IFAC), Via Madonna del Piano 10, I-50019 Sesto Fiorentino, Italy*

[5]*NEST, Istituto Nanoscienze-CNR and Scuola Normale Superiore, Piazza San Silvestro 12, 56127 Pisa, Italy*

[6]*Elettra - Sincrotrone Trieste S.C.p.A., S.S. 14 - km 163, 5 in AREA Science Park, 34149 Basovizza, Trieste, Italy*

[7]*INRS-EMT, Université du Québec, 1650 Boulevard Lionel Boulet, Varennes, Quebec, Canada J3X 1S2*

(Received 23 February 2012; published 30 May 2012)

In heteroepitaxy, impinging beam atoms can either wet the surface or swap with substrate atoms. Herein, we present a dynamic study of these phenomena throughout the assembly of the first atomic layer of Ge on Si(111). *In situ* spectromicroscopic analysis demonstrates that, at a sufficiently high temperature, atom exchange is more significant at the early stages of growth and attenuates as deposition proceeds. Our result highlights the role of propagating monolayer edges in the entropy-driven atom swapping and demonstrates that substitution of Si by Ge is a low-energy pathway to incorporate Ge in the growing monolayer. These observations are confirmed by molecular dynamic simulations.

DOI: 10.1103/PhysRevB.85.201416 PACS number(s): 68.35.bg, 68.37.−d, 68.55.−a

I. INTRODUCTION

The realization of hybrid structures with atomically sharp interfaces has been a formidable challenge in modern materials physics and nanoscience.[1–4] The subject is fundamentally attractive due to the complexity of phenomena involved at the interface between dissimilar materials.[4] From a technological standpoint, the nature and quality of epitaxial interfaces play crucial roles in shaping the properties of hybrid devices and define their functionality and reliability. For the technologically important Ge/Si system, gaining insight and control over the characteristics of the interface is of tremendous significance in the design and fabrication of high-performance electronic and photonic devices.[6,7] It is well established that bulk diffusion (energy barrier of 4–5 eV, Ref. 8) is negligible under typical growth conditions due to kinetic constraints.[9] Thus the competition between Ge surface wetting and Ge-Si swapping across the interface should define the nature of the interface at the initial stage of heteroepitaxy.

The behavior of Ge atoms on Si surfaces has been the subject of extensive experimental and theoretical investigations.[5,10–22] Atomic-scale modeling of Ge growth on Si(001) suggested that entropy limits the wetting tendency of Ge, thus smearing the interface.[18] High-resolution Rutherford backscattering spectrometry (HR-RBS) studies demonstrated that intermixing extends as deep as four layers upon thermal annealing.[12] However, in the Si(111) case, Ge was found to be confined to the two topmost atomic layers, as demonstrated in a recent *in situ* scanning tunneling microscopy (STM) study.[19] In that work Bi-terminated surfaces were used to obtain the chemical contrast between Si and Ge atoms. However, this Bi tagging also influences the intermixing process and hence the composition of the growing monolayer (ML). Although HR-RBS and STM studies unraveled valuable insight into structural and chemical properties of Ge/Si interfaces during sub-ML growth, real-time investigations aiming at a dynamic and quantitative picture of the competition between surface wetting and interface mixing are still missing. The chemical and morphological probes utilized so far involve growth interruptions and quenching[11–13,19] and thus only convey a static description of the interface, which may not disclose its dynamic evolution. Moreover, growth interruption and surface cooling may alter the structural characteristics of the growing ML, as pointed out earlier.[17] In this context, we present a dynamic study of Ge deposition on Si throughout the ML formation at low temperatures. Insights into the atomic processes governing the formation of the Ge/Si interface are obtained by dynamically monitoring both the morphology and composition of the growing ML. We found that the ML growth is nearly abrupt at 200 °C, that is, Ge-Si exchange is rather limited at this temperature. However, an increase in growth temperature up to 270 °C triggers intermixing. This phenomenon is more pronounced at the early stages of the growth of ML-high two-dimensional (2D) islands. By continuing Ge deposition, the extent of intermixing diminishes, and consequently, Ge content progressively increases until it reaches a steady regime. Our observations provide clear evidence for the role of the propagating island edges in atoms swapping across the interface and demonstrate that substitution of Si by Ge is a low-energy pathway to incorporate Ge in the growing one-atom-thick layer. These experimental observations are supported by molecular dynamics (MD) simulations.

II. EXPERIMENTAL DETAILS

Our experiments were carried out using the spectroscopic photoemission and low-energy electron microscope (SPELEEM) at the Nanospectroscopy beam line available at the Elettra synchrotron light source in Trieste. The microscope allows low-energy electron microscopy (LEEM) with a spatial resolution of ∼10 nm and energy-filtered x-ray photoemission electron microscopy (XPEEM) with an energy resolution of ∼0.25 eV. To enable *in situ* investigations of epitaxial

 ©2012 American Physical Society

phenomena, the microscope is equipped with a solid-source molecular beam epitaxy system. The growth was performed by deposition of Ge on Si(111) substrates at a growth rate of $\sim 3.47 \times 10^{12}$ atoms/(cm^2 s) (1.56×10^{15} atoms/cm^2 correspond to 1 ML). Prior to Ge deposition, Si(111) substrates were subjected to extended degassing at 600 °C and then repeatedly heated up to ∼1200 °C until a sharp 1×1 to 7×7 transition was observed. By operating the SPELEEM microscope under the dispersive plane configuration, successive Si $2p$ and Ge $3d$ core-level spectra were dynamically acquired during Ge evaporation from areas of 3-μm diameter using a photon energy of 130 eV.

III. RESULTS AND DISCUSSION

In order to monitor the monolayer formation, LEEM investigations were performed and used as a reference for the dynamic micro x-ray photoelectron spectroscopy (μ-XPS) analysis. Figure 1 displays a representative sequence of a LEEM movie recorded during the ML growth (for the complete movie see the Supplemental Material).[23] The bright contrast corresponds to the ML-high 2D islands. Nucleation of a second layer was never observed in our LEEM data for $\theta < 1$ ML.

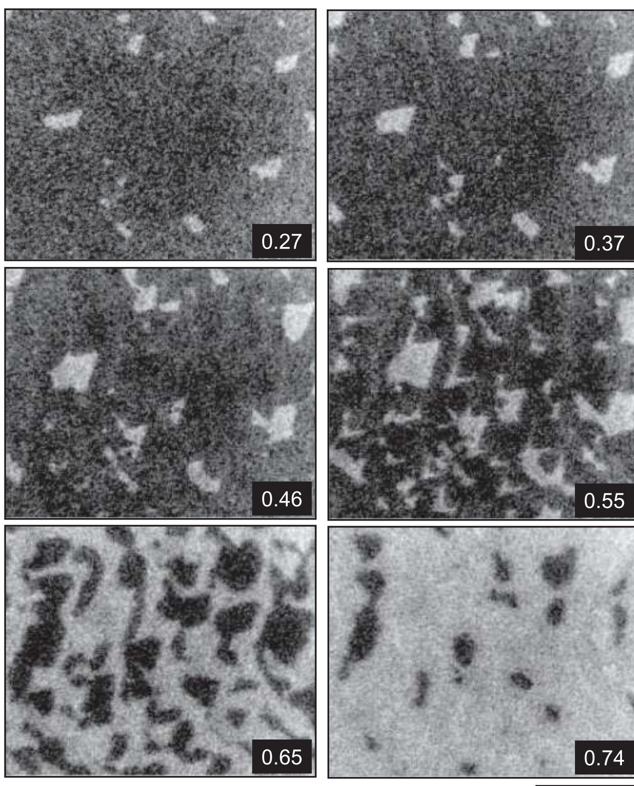

FIG. 1. Sequence of LEEM images showing the nucleation and growth of ML-high 2D islands. Ge coverage (in ML) is indicated at each image. The scale bar denotes 2 μm. Dark areas: bottom layer; bright areas: top layer. Note that the difference in the area covered by the 2D islands and the expected area from the amount evaporated, especially at low coverage, is a consequence of the spatial resolution of LEEM limited to 10 nm. Higher sensitivity to tiny islands is obtained using the integrated intensity of LEEM images.

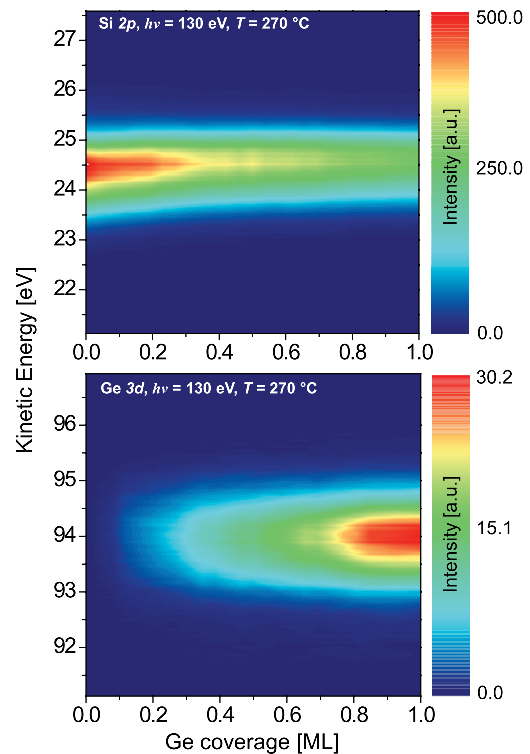

FIG. 2. (Color online) Evolution of (top) Si $2p$ and (bottom) Ge $3d$ core-level spectra during Ge deposition on a Si(111) surface at 270 °C. The spectra were recorded using a photon energy of 130 eV.

The coalescence of 2D islands above ∼0.5 ML leads to the formation of large stripes, which propagate to cover the whole surface after deposition of 1 ML Ge. This growth behavior is independent of temperature in the range investigated in this work (200–270 °C). The morphological changes depicted in Fig. 1 agree well with earlier observations.[14,16,19] Deposited Ge atoms, as well as displaced Si atoms, diffuse towards the islands steps, where they incorporate. However, as inferred below, the growth may involve more complex atomic pathways.

On samples identical to those investigated by LEEM, Si $2p$ and Ge $3d$ core-level spectra were recorded during Ge deposition until completion of the ML growth. Figure 2 displays the Si $2p$ and Ge $3d$ intensity maps measured throughout the ML assembly at 270 °C. Expectedly, the intensity of the Ge $3d$ peak progressively increases with Ge deposition, whereas the intensity of the Si $2p$ peak decreases due to the attenuation of the photoelectron signal by the growing layer. The theoretical XPS intensity can be calculated using the Berglund and Spicer treatment,[24] which gives the intensity of the photoelectron flux from element α perpendicular to the sample surface emitted from the volume element dV at a depth h as $dI = I_0 N x_\alpha \sigma_\alpha e^{-h/\lambda_\alpha} dV$, where x_α, σ_α, and λ_α are elemental concentration, photoemission cross section, and photoelectron escape depth, respectively. N is the atomic density, and I_0 accounts for the x-ray intensity and photoelectron detection efficiency. Considering the general case of n SiGe intermixed layers ($n \geqslant 1$) on a Si substrate, the intensity of the Si $2p$ core level ($I_{\mathrm{Si}2p}$) includes the contributions from Si atoms in these n layers; that from the

buried Si substrate; and that from bare Si substrate, i.e., from those regions which are not yet covered by the 2D islands and which we assume to be stable against Ge incorporation or adsorption.[25] On the other hand, the intensity of the Ge $3d$ core level ($I_{\mathrm{Ge}3d}$) originates from the n intermixed layers. Atoms hopping on the Si surface are treated as single-atom 2D islands. From this, at any Ge coverage (θ), $I_{\mathrm{Si}2p}(\theta)$ and $I_{\mathrm{Ge}3d}(\theta)$ read

$$I_{\mathrm{Si}2p}(\theta) = I_0 N \sigma_{\mathrm{Si}} \lambda_{\mathrm{Si}} \left\{ 1 - A(\theta) + A(\theta) \left[e^{-nh/\lambda_{\mathrm{Si}}} + \sum_{i=1}^{n} x_i^{\mathrm{Si}} \left(e^{-(i-1)h/\lambda_{\mathrm{Si}}} - e^{-ih/\lambda_{\mathrm{Si}}} \right) \right] \right\}, \quad (1)$$

$$I_{\mathrm{Ge}3d}(\theta) = I_0 N \sigma_{\mathrm{Ge}} \lambda_{\mathrm{Ge}} A(\theta) \sum_{i=1}^{n} x_i^{\mathrm{Ge}} \left(e^{-(i-1)h/\lambda_{\mathrm{Ge}}} - e^{-ih/\lambda_{\mathrm{Ge}}} \right), \quad (2)$$

where $A(\theta)$ is the surface fraction covered by the ML-high 2D islands and h is the thickness of an atomic layer. x_i^{Ge} and x_i^{Si} ($x_i^{\mathrm{Ge}} + x_i^{\mathrm{Si}} = 1$ and $\sum_{i=1}^{n} x_i^{\mathrm{Ge}} = 1$) denote the Ge and Si concentrations of layer i, respectively. In the limit of an abrupt interface featuring a pure Ge ML on Si substrate (i.e., $n = 1$, $x_1^{\mathrm{Ge}} = 1$, and $x_1^{\mathrm{Si}} = 0$), the corresponding intensity ratio $\frac{I_{\mathrm{Ge}3d}(\theta)}{I_{\mathrm{Si}2p}(\theta)}$ is given by

$$\Re_{\mathrm{abrupt}}(\theta) = \frac{I_{\mathrm{Ge}3d}(\theta)}{I_{\mathrm{Si}2p}(\theta)} = \frac{\sigma_{\mathrm{Ge}}}{\sigma_{\mathrm{Si}}} \frac{\lambda_{\mathrm{Ge}}}{\lambda_{\mathrm{Si}}} \frac{A(\theta)\left(1 - e^{-h/\lambda_{\mathrm{Ge}}}\right)}{1 - A(\theta)\left(1 - e^{-h/\lambda_{\mathrm{Si}}}\right)}. \quad (3)$$

Figure 3(a) displays the evolution of $\Re_{\mathrm{abrupt}}$ as a function of θ (solid line). $A(\theta)$ is estimated from LEEM images. The experimental intensity ratios of core-level spectra acquired at 200 and 270 °C are also shown (dots). Independent of θ, $\Re_{\mathrm{abrupt}}$ differs significantly from the experimental data recorded at 270 °C. Here we ascribe this discrepancy to intermixing with Si substrate atoms. This intermixing is rather limited at 200 °C, as indicated by an intensity ratio very close to $\Re_{\mathrm{abrupt}}$. Note that the absence of a significant intermixing in earlier growth experiments performed at temperatures much higher than those used in this work is attributed to Bi being used as a marker in STM analysis.[19] Indeed, Bi, which acts as a surfactant, floats on the top of the growing layer and suppresses the intermixing of Si and Ge.[26] Figure 3(b) exhibits the evolution of the relative variation of the ratio of core-level intensities with respect to the abrupt growth ratio (defined as $\delta\Re = \frac{\Re_{\mathrm{abrupt}}(\theta) - \Re(\theta)}{\Re_{\mathrm{abrupt}}(\theta)}$). Herein, $\delta\Re$ provides a dynamic and semiquantitative measurement of the degree of exchange between substrate atoms and deposited atoms. It is noteworthy that $\delta\Re$ is not sensitive to θ ($\delta\Re_{200^\circ\mathrm{C}} \sim 0.1$) at the lowest growth temperature. This suggests that the assembled 2D islands keep the same elemental composition throughout the growth. At 270 °C, $\delta\Re$ evolves remarkably differently. First, it decreases monotonously at the early stage of the growth and then becomes practically unchanged ($\sim$0.3) for $\theta \geqslant \sim$0.4 ML, indicating a stable composition of the growing 2D islands; that is, the incorporation of Si and Ge takes place at the same rate in this regime. The interesting fact here is, however, the gradual decrease in $\delta\Re$, which is explained by a continuous increase in Ge content as the 2D islands grow larger for $\theta \leqslant 0.4$ ML.

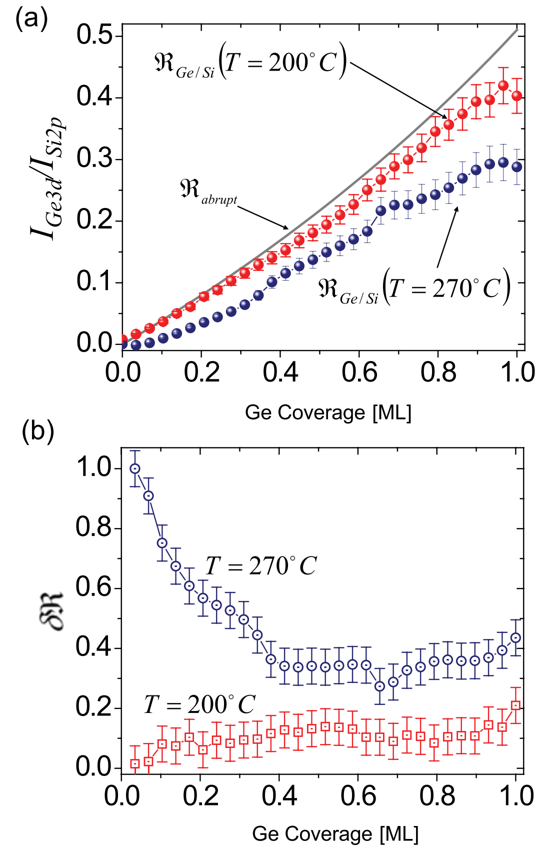

FIG. 3. (Color online) (a) Variation of Ge $3d$ to Si $2p$ intensity ratios as a function of Ge coverage. The solid line corresponds to the calculated values for an abrupt Ge/Si interface ($\Re_{\mathrm{abrupt}}$) and dots are the experimental data recorded during growth. (b) Evolution of $\delta\Re$ as a function of Ge coverage at growth temperature of 200 °C (squares) and 270 °C (circles).

The observations above suggest that intermixing progressively slows down as the growth proceeds. One may invoke two competing pathways of atomic mixing to explain these processes. First, in the low-coverage regime ($\theta \leqslant 0.4$ ML at 270 °C), Ge deposition produces scattered 2D islands on the Si(111) surface (Fig. 1). These islands display a high rim length-to-surface area ratio, which may promote substantial Si incorporation. Indeed, earlier reports have pointed out the critical role of step edges in Ge-Si intermixing.[17,19] Thus it is reasonable to expect these 2D islands to contain a substantial amount of Si due to the exchange process promoted by the relative importance of the rim-to-surface ratio. Here, the fact that the atoms at the island edges have fewer nearest neighbors provides them with more steric freedom for an exchange process. As Ge coverage increases, the 2D islands enlarge and begin to coalesce (Fig. 1), thus forming larger islands with a lower rim-to-surface ratio and hence a smaller relative importance of Ge-Si exchanges at island edges. Second, the expanding fraction of surface covered implies an increasing probability for Ge atoms to be directly deposited onto these 2D islands. Here, the impinging Ge atoms can

incorporate into the growing 2D islands through trapping at step edges. Alternatively, following a displacive adsorption mechanism,[27,28] Ge atoms deposited directly on the growing layer can remove Si and Ge atoms and occupy their sites. The displaced atoms can diffuse on the surface and possibly attach to step edges. In this latter scenario, only the substitution of Si atoms induces an increase in Ge content. To verify the consistency of these mechanisms, we investigated the evolution of the 2D islands by MD simulations.

MD simulations were performed using a $28.22 \times 23.04 \times 39.93$ Å^3 Si supercell and an improved bond-order potential (BOP4+).[29] This potential is based on the tight-binding model and preserves the essential quantum-mechanical nature of atomic bonding. Calculations of atomic displacements, potential energy, stress, and temperature were done in 0.5-fs steps. The system was allowed to equilibrate, both geometrically and compositionally, before being subjected to annealing up to ∼270 °C. During the cooling, the system relaxes through atomic displacements and volume changes. The simulated deposition of Ge atoms on a Si(111) surface demonstrates the nucleation of alloyed ML-high 2D islands with very negligible adsorption on bare Si (less than 1% of deposited atoms), and intermixing is found to be predominantly confined in the two topmost layers, in agreement with earlier observations.[19] Here, the lower surface diffusivity and denser double-layer structure of Si(111) may be at the origin of this limited mixing as opposed to Si(100), where Ge can reach down to the fourth layer.[12,18] Various configurations accounting for different Ge and Si distributions within the 2D islands were computed. Figure 4 displays a representative set of simulated configurations with $x_1^{\mathrm{Ge}} \sim 0.5$. The analysis of the distribution of atoms and of the nature of interatomic bonds in the simulated configurations indicates that, within the range of a maximum of 1.3 of the equilibrium covalent bond distance of approximately Si-Si = 2.351 Å, Ge-Ge = 2.447 Å, and Si-Ge = 2.398 Å, all atoms have two (atoms at the edge in the surface layer), three (surface-layer atoms far from the edge), or four (buried atoms) bonds. It is noteworthy that the measured bond length is characteristic for double bonds in nonfourfold bonding situations, which is indicative of surface reconstruction. For comparison, a 2D island was also simulated in the absence of relaxation [Fig. 4(a)]. At equilibrium, the calculated potential energy E_{POT} in this case was estimated at ~ -4.288 eV/atom. To minimize the stress, a significant distortion of the lattice in surface and subsurface layers takes place during relaxation parallel to a rearrangement of surface layer atoms. This reduces E_{POT} by ∼50–70 meV/atom. An additional gain of ∼60–70 meV/atom is obtained after deposition and entrapment of a Ge atom at the edges. Figures 4(c) and 4(d) display the evolution of the 2D island after addition of a Ge atom. This atom displaces an existing Si atom, which was allowed to freely diffuse on the surface. For all investigated configurations, we observed two distinct scenarios with the displaced Si atom either diffusing away or attaching to the 2D island step edges. In this latter case, E_{POT} drops by ∼7 to ∼16 meV/atom. Instead, the decrease is only ∼6 to ∼8 meV/atom when the displaced Si atom diffuses away. In both cases the decrease of E_{POT} indicates that the substitution of Si by newly deposited Ge is a low-energy pathway for the Ge enrichment of the growing alloyed ML, which supports the mechanisms proposed above.

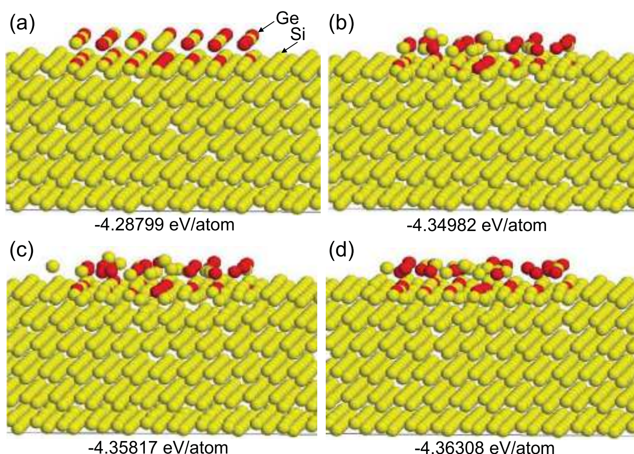

FIG. 4. (Color online) Side view (with a 5° inclination) of the distribution of atoms obtained by MD simulations: (a) the initial $\mathrm{Si_{0.5}Ge_{0.5}}$ 2D island and (b) the 2D island in (a) after annealing at 250 °C, (c) after deposition of a Ge atom with displaced Si detached from the 2D island, and (d) after deposition of a Ge atom with displaced Si attached to the step edge. The corresponding potential energies are indicated. Note that in (b)–(d) atoms are allowed to leave their lattice sites.

IV. CONCLUSION

In conclusion, we have presented a dynamic probe of atomic mixing throughout the assembly of a single ML during the epitaxy of Ge on Si(111). We developed an analytical model to assess the exchange between substrate atoms and deposited atoms in a one-atomic-layer-thick 2D island during their assembly and coalescence. Intermixing with substrate atoms was found to be sensitive to substrate temperature. At 200 °C, the deposited atoms were found to predominantly wet the surface, whereas at 270 °C the intermixing is stronger especially at the early growth stages. By continuing Ge deposition at this temperature, Ge surface content progressively increases parallel to lateral growth of 2D islands to form one atomic layer. Our observations provide evidence for the role of the propagating 2D island edges in the entropy-driven atomic swapping, whereas the expanding terraces resulting from coalescence of fragmented 2D islands become favorable sites for Ge incorporation.

ACKNOWLEDGMENTS

O.M. is grateful to B. Voigtländer for valuable discussions and to JSPS, BMBF (Contracts No. 01BU0624 and No. 13 N 9881), and NSERC for financial support. The authors thank T. O. Mentes for the help in capturing XPS and LEEM data. F.R. acknowledges funding from NSERC and is grateful to the Canada Research Chairs program for partial salary support.

*Oussama.moutanabbir@polymtl.ca

[1] J. Robertson, Solid State Electron. **49**, 283 (2005).
[2] J. Matsui and J. Mizuki, Annu. Rev. Mater. Sci. **23**, 295 (1993).
[3] F. Schäffler, Semicond. Sci. Technol. **12**, 1515 (1997).
[4] N. Akagawa, H. Y. Hwang, and D. A. Muller, Nat. Mater. **5**, 204 (2006).
[5] T. Leontiou, J. Tersoff, and P. C. Kelires, Phys. Rev. Lett. **105**, 236104 (2010).
[6] *SiGe, Ge, and Related Compounds 4: Materials, Processing, and Devices*, ECS Trans. Vol. 33(6), edited by D. Harame, J. Boquet, M. Östling, Y. Yeo, G. Masini, M. Caymax, T. Krishnamohan, B. Tillack, S. Bedell, S. Miyazaki, A. Reznicek, and S. Koester (2010).
[7] J. Michel, J. Liu, and L. C. Kimerling, Nat. Photonics **4**, 527 (2010).
[8] P. Dorner, Philos. Mag. **49**, 557 (1984).
[9] J. Tersoff, Phys. Rev. Lett. **74**, 5080 (1995).
[10] J. A. Carlisle, T. Miller, and T. C. Chiang, Phys. Rev. B **49**, 13600 (1994).
[11] L. Patthey, E. L. Bullock, T. Abukawa, S. Kono, and L. S. O. Johansson, Phys. Rev. Lett. **75**, 2538 (1995).
[12] K. Nakajima, A. Konishi, and K. Kimura, Phys. Rev. Lett. **83**, 1802 (1999).
[13] B. P. Uberuaga, M. Leskovar, A. P. Smith, H. Jonsson, and M. Olmstead, Phys. Rev. Lett. **84**, 2441 (2000).
[14] J.-H. Cho and M.-H. Kang, Phys. Rev. B **61**, 1688 (2000).
[15] F. Rosei, N. Motta, A. Sgarlata, G. Capellini, and F. Boscherini, Thin Solid Films **369**, 29 (2000).
[16] D. S. Lin, J. L. Wu, S. Y. Pan, and T. C. Chiang, Phys. Rev. Lett. **90**, 046102 (2003).
[17] J. B. Hannon, M. Copel, R. Stumpf, M. C. Reuter, and R. M. Tromp, Phys. Rev. Lett. **92**, 216104 (2004).
[18] R. J. Wagner and E. Gulari, Phys. Rev. B **69**, 195312 (2004).
[19] N. Paul, S. Filimonov, V. Cherepanov, M. Cakmak, and B. Voigtländer, Phys. Rev. Lett. **98**, 166104 (2007).
[20] M. Brehm, M. Grydlik, H. Lichtenberger, T. Fromherz, N. Hrauda, W. Jantsch, F. Schäffler, and G. Bauer, Appl. Phys. Lett. **93**, 121901 (2008).
[21] O. Moutanabbir, S. Miyamoto, E. E. Haller, and K. M. Itoh, Phys. Rev. Lett. **105**, 026101 (2010).
[22] E. Bussmann and B. S. Swartzentruber, Phys. Rev. Lett. **104**, 126101 (2010).
[23] See Supplemental Material at http://link.aps.org/supplemental/10.1103/PhysRevB.85.201416 for the complete LEEM movie of Fig. 1.
[24] C. N. Berglund and W. E. Spicer, Phys. Rev. **136**, 1030 (1964).
[25] R. Schorer, E. Friess, K. Eberl, and G. Abstreiter, Phys. Rev. B **44**, 1772 (1991).
[26] M. Horn-von Hoegen, Appl. Phys, A **59**, 503 (1994).
[27] Y. L. Wang, H.-J. Gao, H. M. Guo, S. Wang, and S. T. Pantelides, Phys. Rev. Lett. **94**, 106101 (2005).
[28] R. M. Tromp, Phys. Rev. B **47**, 7125 (1993).
[29] V. Kuhlmann and K. Scheerschmidt, Phys. Rev. B **76**, 14306 (2007).